Digital Object Identifier (DOI): 10.1109/PTC.2015.7232799

PowerTech, 2015 IEEE Eindhoven, 29th June - 2nd July 2015

Coordinated Frequency and Voltage Overload Control of Smart Transformers

Giovanni De Carne
Giampaolo Buticchi
Marco Liserre
Panagiotis Marinakis
Costas Vournas

Suggested Citation

G. De Carne, G. Buticchi, M. Liserre, P. Marinakis and C. Vournas, "Coordinated frequency and Voltage Overload Control of Smart Transformers," *2015 IEEE Eindhoven PowerTech*, Eindhoven, 2015, pp. 1-5.

Coordinated Frequency and Voltage Overload Control of Smart Transformers

Giovanni De Carne
Giampaolo Buticchi
Marco Liserre
Chair of Power Electronics
Christian Albrechts University of Kiel
Kiel, Germany
gdc@tf.uni-kiel.de

Panagiotis Marinakis
Costas Vournas
School of Electrical and Computer Engineering
National Technical University of Athens
Athens, Greece
marinakispanagiotis@gmail.com
vournas@power.ece.ntua.gr

***Abstract*—A Smart Transformer (ST) is a power electronics-based transformer that aims not only to substitute the traditional transformer but to upgrade also the LV and MV grid. In order to limit the costs, the ST must be carefully designed, constraining the current carried by the ST. In this paper a Combined Frequency and Voltage Controller is proposed, in order to manage a possible overload without derating the ST. Aiming to reduce the current, this control enhances the ST security against the overload situation interacting with the local Distributed Generation (DG) and the local loads.**

***Index Terms*—Overcurrent Limitation - Overload control - Voltage Control - Smart Transformer - Solid State Transformer**

I. Introduction

The Smart Transformer (ST), based on power electronics [1], can provide new grid services and enable new promising way for optimizing the grid operations. The ST features for the Low (LV) and Medium Voltage (MV) grid have been described in a companion paper [2] and in [3]. As stated, one key problem lies on the control of ST current so that it does not exceed the safe operation limits. In [2] we considered a controller able to change the frequency in order to obtain assistance from the controlled distributed generation sources connected to the LV grid for lowering the transformer current.

The present paper addresses the case where the amount of energy or power available in the controlled distributed generation sources is not sufficient for dealing with the transformer overload condition. For this reason, we propose a different control scheme including both frequency and voltage control. The proposed controller aims to use the voltage sensitivity of the load in order to manage the high current flowing in the ST, in case the frequency control is ineffective. Following the techniques and the terminology used in microgrids [4]–[6], a master controller is implemented in the ST and a frequency-active power droop controller is installed at the DG converter site.

In this work a PhotoVoltaic (PV) plant equipped with a Battery Energy Storage System (BESS) is assumed as controllable distributed energy resource. The BESS contributes to limit the power fluctuation in the feeder and thus to increase the PV integration in the grid [7]–[9]. Fig. 1 describes the concept of the Coordinate Frequency and Voltage Overload Control. It depicts the control possibilities offered depending on the amount of controllable DG integrated in the grid. For as long as the ST current is in the safe operation region (i.e. far from the limit), both voltage and frequency of the master controller are set to nominal values (OS I). When the ST current approaches its limit and the amount of controllable DG is sufficient for frequency regulation, the master controller changes the frequency requesting the assistance from the DG droop controller (OS II). When the DG is not sufficient to control frequency, or the allowable frequency variation limit is reached, the master controller starts decreasing the voltage level at the LV terminal of the ST: considering voltage sensitive loads connected to the grid, the transformer overload is avoided (OS III).

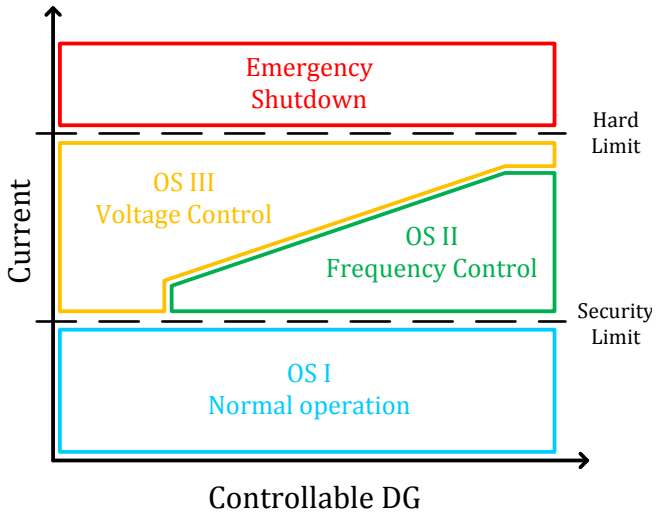

Fig. 1. Coordinate Frequency and Voltage Overload Control Concept: control action performed depending on the amount of controllable DG integrated in the grid

This paper is structured as follows: Section II presents the Combined Frequency and Voltage Overload controller; Section III describes the benchmark grid; Section IV explains the

steady state behavior of the Frequency-Voltage Controller and Section V shows the dynamic simulation results. Finally, the conclusions are drawn in Section VI.

II. Frequency and Voltage Overload Control

The controller described in this paper is composed of a master controller, managed by the ST, and droop controllers at the DG interfaces with the LV grid.

In Operating stage I (OS I), already shown in Fig. 1, both frequency and voltage are kept constant at their respective set-points, working in the normal operation conditions. In OS II the master controller keeps the voltage constant, but modifies the grid frequency thus activating the f-P droop controllers of the DG. In OS III the master controller decreases the voltage magnitude, when the OS II response is not sufficient to keep the current below the set limit. Essentially, this is achieved by modifying the LV converter control logic: instead of controlling the voltage at the grid side, the converter controls the current value modifying the voltage values.

The overall controller scheme is shown schematically in Fig. 2.

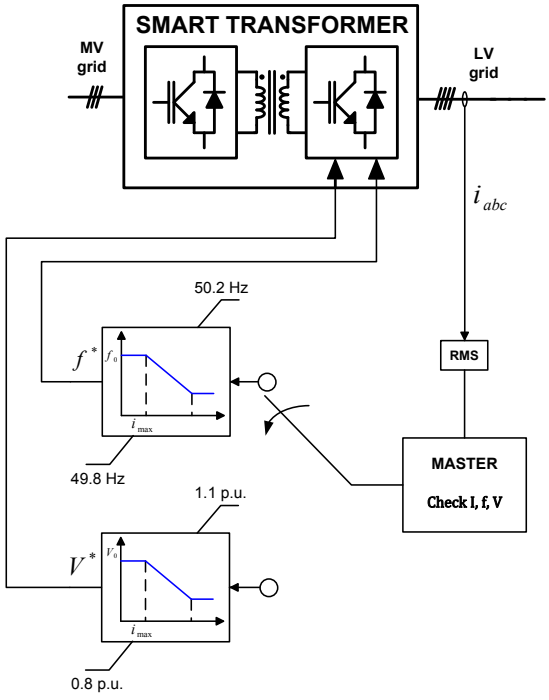

Fig. 2. Master controller of the ST

The schematic working procedure that is implemented at every time step is depicted in the flow chart of Fig. 3. The master controller checks continuously the current injection in the LV grid. If the current reaches the security alert limit, it enables the frequency controller. If the frequency controller action has reached a limit due to the low amount of stored energy in the DG, or due to the maximum permissible frequency variation (here fixed to 49.8Hz), the master controller enables the voltage level control. Governing the injection of active power of the DG, the frequency controller has a limited capability in terms of energy stored, but its impact on the grid quality of service is negligible, so it must be preferred as the first solution in case of overload. On the other hand, the voltage control works directly on the master controller to limit the current. Assuming a voltage sensitive load (in this paper constant impedance is assumed throughout), the load current tends to decrease when the voltage decreases. This control is used only in case of emergency, due to the strong impact on the quality of service. Here a lower voltage limit of 0.8 p.u. has been implemented to avoid the electrical appliances shutdown.

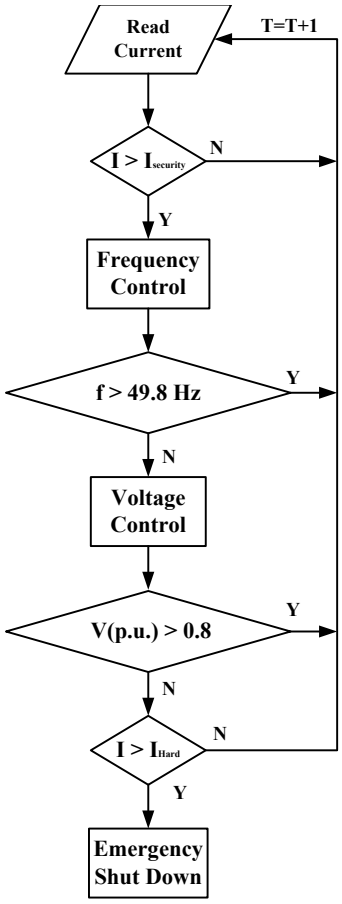

Fig. 3. Controller Flow Chart

The first level of emergency control (OS II) is enabled as soon as the master controller measures the current above the security limit. This method has been described in the companion work with an asynchronous generator [2], and it is now applied to a Batteries Energy Storage System (BESS), which is installed in the Distributed Generation (DG) site. The BESS has limited capability: the amount of power and energy that the batteries can provide depends on the the battery size and the available State Of Charge (SOC) respectively. If the load grows so that the batteries charge is depleted, the frequency control cannot anymore solve the overload.

When the limits of available DG/BESS control have been exhausted, the frequency is kept constant and the voltage is

lowered so that the current remains within the limits (OS III). Under the hypothesis of constant impedance nature of the loads, the current is directly proportional to the voltage. Once the overload is solved and the current goes below the security limit, the master controller disables the emergency control, so that the ST comes back to the normal operative conditions.

III. Benchmark Grid

The simulated grid is represented by a simple radial, two lines, three bus system, as shown in Fig. 4. The system is composed of an aggregate passive load, a PV power plant equipped with a BESS and the ST. The BESS is used to regulate frequency when needed, in order to facilitate the grid integration of the PV. The PV active power injection is assumed to be constant at 50 kW in this system. The BESS/DG converter maximum power is taken equal to 70 kVA. A constant power factor $cos\varphi = 1$ has been assumed in the AC side of the BESS/DG converter controller for the simulations.

The software implementation of the ST has been already described in [2]. The battery/DG converter has been modeled as a Current Controlled - Voltage Source Converter (CC-VSC), with a switching frequency of 5kHz. The simulations have been performed in PSCAD/EMTDC® with a time step of 20μs.

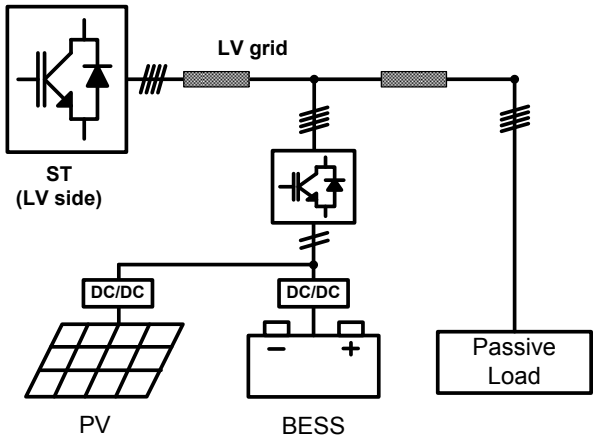

Fig. 4. Benchmark Grid

The active power control of the batteries/DG system is achieved by means of a frequency droop controller. The controller receives the frequency signal from the grid and compares it with the rated frequency value. The error is sent to a proportional controller that determines the power contribution of the droop controller to the active power rated value. When the ST changes the grid frequency in the Operating Stage II, the batteries increase the injected power trying to compensate the frequency variation.

IV. Steady State Operating Regions

This section describes the steady state operations of the proposed controller for different load demand levels. Fig. 5 shows the impact on active power, transformer secondary side (LV) rms voltage and current in the proposed grid of the load admittance increase, assuming a succession of steady state conditions.

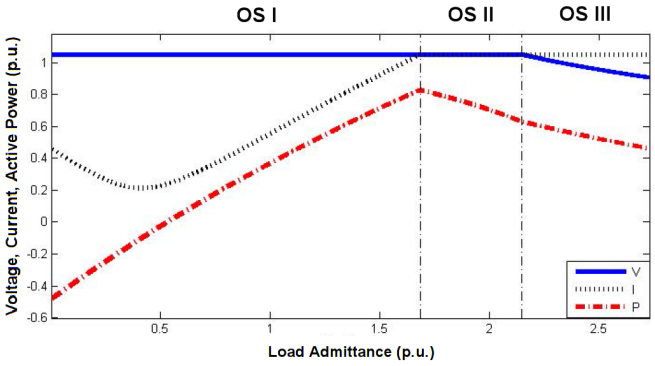

Fig. 5. Operating Stages: rms voltage (continue blue line), rms current (dashed black line), active power (dash-dot red line)

As already discussed, the proposed controller operation is divided in 3 Operating Stages (OS):

OS I: the current values in the ST are within the range of the ordinary operating conditions. The voltage in the transformer secondary is set to a predefined set-point value (in this case 1.05 p.u.) and thus the transformer apparent power increases linearly with the current. Note in Fig. 5 that for load demand below the assumed PV generation (i.e., 0.5 pu) the active power becomes negative, i.e. it flows from the LV to the MV transformer side, thus the transformer current is reduced as the feeder load increases. When the active load (plus losses) equals the PV generation, the transformer active power becomes zero and at this point the current is purely reactive. After that rms current increases with load demand.

OS II: the current has gone above the safety threshold (1.05 p.u.), thus the ST decreases the grid frequency and the f-P droop controller drives the DG to increase its active power injection. Consequently, the active power injected by the ST decreases, and the rms current value is kept constant at the desired security threshold.

OS III: when the minimum frequency value allowable is reached (or the DG has reached its rated power, or depleted its energy reserve), the ST keeps the feeder current constant at the specified security value, thus the voltage drops with increasing load demand. Note that this causes also the active power to drop meaning that the requested load demand is not met.

Clearly, in Operating State III service quality to the consumers is degraded in order to avoid the disconnection of the transformer leading to feeder blackout.

V. Simulation Results

This Section aims to demonstrate the effective coordination of the 3-stage controller for the management of the overload. The aggregate load demand is increased in a short-term time

window, changing from 550kW to 700kW in 30 seconds, keeping the power factor equal to 0.9, as shown in Fig. 6.

Considering the constant impedance nature of the load, as soon as the load power demand increases, the current flowing through the ST increases as well. The controller notices the current increase and as soon as the current value goes above the security limit, it switches to the appropriate operating stage. In Fig. 7, despite the fast load power transient, the overload is well managed by the controller and the current always lies below the current hard limit. The switches from OS I to OS II and from OS II to OS III are clearly visible in the Figure: despite the linear load increase, the current increase changes slope, meaning that the controller entered in OS II and the droop controller is interacting with the frequency change. When the controller enters in OS III, the current is kept constant and both voltage and consumed power decrease. When the load demand begins to decrease after 50s so that the requested transformer current reduces below the Security Limit, the controller switches back in the OS II. There is a small increase of the current due to the change from the frequency to the voltage controller, but the current flow is well managed till the end of the load transient.

The aforementioned considerations are also shown in Fig. 8. The load, operating as a constant impedance, consumes less power with respect to its demand: the drop of voltage in the line reduces the voltage at load level and thus the power provided to the load decreases as well. Consequently the power consumed is less than the one demanded, as can be seen by comparing with Fig. 6. By decreasing voltage during the OS III, the power peak has been shaved by the controller, reducing the current peak as seen in Fig. 7. As it can be seen also in Fig. 8 this method has a considerable impact on the load served. Therefore, the voltage controller of OS III must be tuned properly, in order to avoid excessive decrease in power quality.

A more detailed description of the controllers operations is present in Fig. 9, 10, 11.

As soon as the current goes above the security limit imposed, the controller enters in OS II. Here the master controller modifies the voltage waveform frequency, as described in Fig. 9, in order to interact with the droop controller at BESS level. The BESS controller, measuring a frequency drop, increases the active power injection of the BESS (Fig. 10), until it reaches the maximum available active power. In contrast with [2], the amount of energy and power available in this case are not sufficient to overcome the overload situation.

When the BESS reaches the maximum power injection limit after 35 seconds, the frequency controller drops instantaneously the frequency, hitting the control lower limit, as can be noticed in Fig. 9.

Thus, the master controller detects the OS III: the frequency has already reached the minimum value, due to the insufficient power contribution by the BESS, and it switches to the voltage control. Here the voltage is decreased (Fig. 11) and the current stays near the security limit (Fig. 7). As soon as the current decreases below the security limit, the voltage controller returns to the normal operation setpoint, and the frequency controller takes over again, in order to regulate the current through the ST by modifying DG active power. After a small transient caused by the switch between the controllers, the frequency controller continues to keep the current under control, till the end of the load transient.

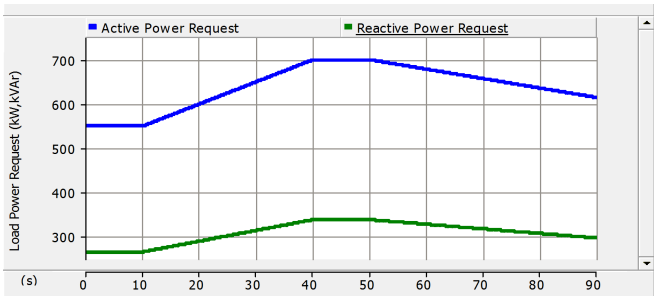

Fig. 6. Load active (blue line) and reactive (green line) power requested by the load

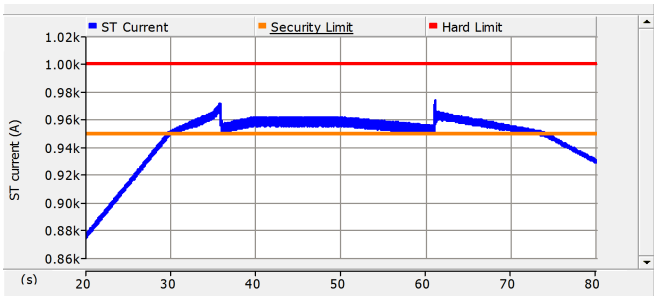

Fig. 7. Current flowing in the ST (blue line), Current Security Limit (orange line), Current Hard Limit (red line) in case of Frequency and Voltage Overload Control application

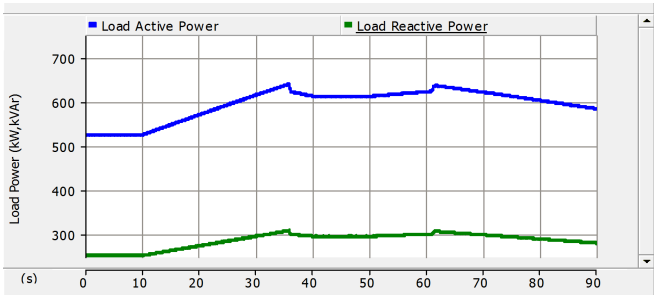

Fig. 8. Active (blue line) and Reactive (green line) Power absorbed by the load when the control is applied

VI. Conclusion

The Smart Transformer represents a promising technologies for the development of the LV and MV grids of the future. It is able to perform the same tasks of the traditional transformer, providing at the same time new services. However the ST higher realization costs do not allow to oversize the power electronics components, thus it reduces the overload capability during load peaks. This work has depicted a promising control

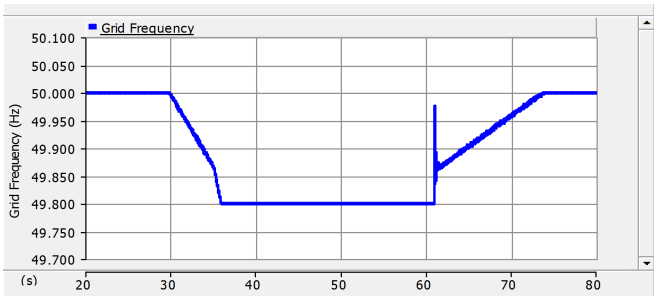

Fig. 9. Grid frequency during the load transient

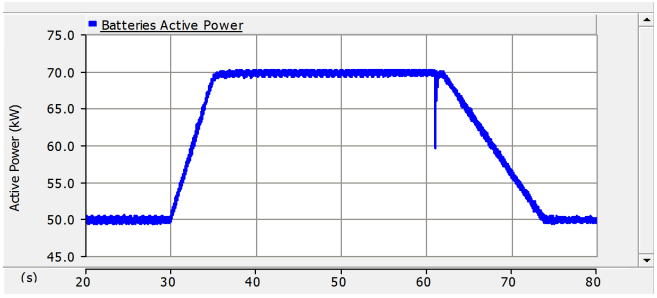

Fig. 10. BESS Active Power during the load transient

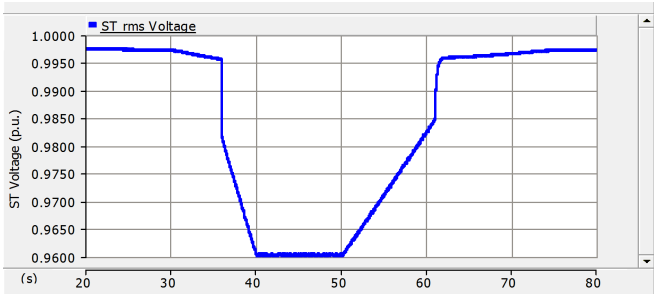

Fig. 11. rms Voltage at ST level during the load transient

possibility for avoiding the ST overload problem. In presence of limited DG capability, this Coordinated Voltage-Frequency Overload Control is more effective than the simple frequency control described in [2]. The frequency control impacts very little on the quality of the service, but it has a limited action range, in which it is effective. On the contrary, the voltage control is very fast and it is always effective (provided that load is voltage sensitive), but it impacts more on the service quality.

ACKNOWLEDGMENT

The research leading to these results has received funding from the European Research Council under the European Union's Seventh Framework Programme (FP/2007-2013) / ERC Grant Agreement n. [616344] - HEART.

REFERENCES

[1] R. Pena-Alzola, G. Gohil, L. Mathe, M. Liserre, and F. Blaabjerg, "Review of modular power converters solutions for smart transformer in distribution system," in *IEEE Energy Conversion Congress and Exposition (ECCE)*, Sept 2013, pp. 380–387.

[2] G. De Carne, G. Buticchi, M. Liserre, and C. Vournas, "Frequency-based overload control of smart transformer," in *IEEE Power Tech*, 2015.

[3] G. De Carne, G. Buticchi, M. Liserre, C. Yoon, and F. Blaabjerg, "Voltage and current balancing in low and medium voltage grid by means of smart transformer," in *IEEE PES GM*, 2015.

[4] J. Peas Lopes, C. Moreira, and A. Madureira, "Defining control strategies for analysing microgrids islanded operation," in *IEEE Power Tech*, June 2005, pp. 1–7.

[5] F. Katiraei, M. Iravani, and P. Lehn, "Micro-grid autonomous operation during and subsequent to islanding process," *IEEE Transactions on Power Delivery*, vol. 20, no. 1, pp. 248–257, Jan 2005.

[6] G. Diaz, C. Gonzalez-Moran, J. Gomez-Aleixandre, and A. Diez, "Scheduling of droop coefficients for frequency and voltage regulation in isolated microgrids," *IEEE Transactions on Power Systems*, vol. 25, no. 1, pp. 489–496, Feb 2010.

[7] X. Li, D. Hui, and X. Lai, "Battery energy storage station (bess)-based smoothing control of photovoltaic (pv) and wind power generation fluctuations," *IEEE Transactions on Sustainable Energy*, vol. 4, no. 2, pp. 464–473, April 2013.

[8] Y. Riffonneau, S. Bacha, F. Barruel, and S. Ploix, "Optimal power flow management for grid connected pv systems with batteries," *IEEE Transactions on Sustainable Energy*, vol. 2, no. 3, pp. 309–320, July 2011.

[9] C. Hill, M. Such, D. Chen, J. Gonzalez, and W. Grady, "Battery energy storage for enabling integration of distributed solar power generation," *IEEE Transactions on Smart Grid*, vol. 3, no. 2, pp. 850–857, June 2012.